ACS APPLIED MATERIALS & INTERFACES

Research Article

www.acsami.org

Highly Sensitive and Selective Sensor Chips with Graphene-Oxide Linking Layer

Yury V. Stebunov,*[,†] Olga A. Aftenieva,[†] Aleksey V. Arsenin,[†] and Valentyn S. Volkov[†,‡]

[†]Laboratory of Nanooptics and Plasmonics, Moscow Institute of Physics and Technology, 9 Institutsky Lane, Dolgoprudny 141700, Russian Federation

[‡]Institute of Technology and Innovation, University of Southern Denmark, Campusvej 55, DK-5230 Odense M, Denmark

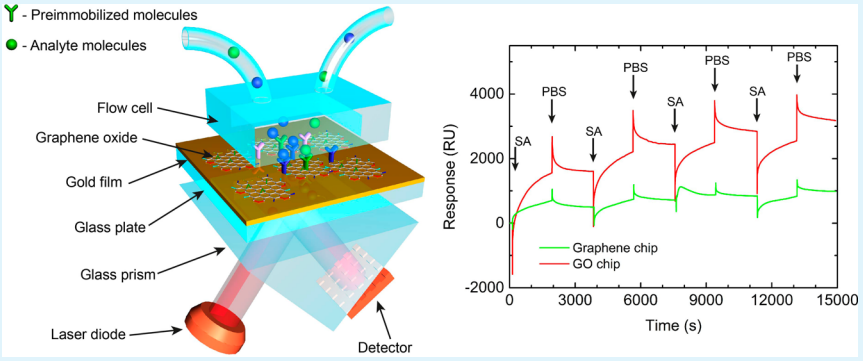

ABSTRACT: The development of sensing interfaces can significantly improve the performance of biological sensors. Graphene oxide provides a remarkable immobilization platform for surface plasmon resonance (SPR) biosensors due to its excellent optical and biochemical properties. Here, we describe a novel sensor chip for SPR biosensors based on graphene-oxide linking layers. The biosensing assay model was based on a graphene oxide film containing streptavidin. The proposed sensor chip has three times higher sensitivity than the carboxymethylated dextran surface of a commercial sensor chip. Moreover, the demonstrated sensor chips are bioselective with more than 25 times reduced binding for nonspecific interaction and can be used multiple times. We consider the results presented here of importance for any future applications of highly sensitive SPR biosensing.

KEYWORDS: *surface plasmon resonance, graphene, graphene oxide, sensor chips, sensing interface*

1. INTRODUCTION

Biosensing based on surface plasmon resonance (SPR) is widely used today to investigate biochemical reactions in scientific and pharmaceutical research, food research, and medical diagnostics.[1] In particular, SPR provides biosensing without requiring fluorescent, radioactive, or other types of labeling, which could interfere with the biosensing process, sensitivity, and real-time monitoring of biomolecule binding. Therefore, label-free SPR-based biosensing allows measurement of the adsorption and desorption coefficients.[2,3] However, SPR-based biosensing has a lack of sensitivity for applications with small molecules and low concentrations of analyte.[3] To improve the biosensing performance, researchers have proposed different optical structures for SPR sensor chips[4−8] as well as different immobilization techniques.[9−12] Gold has been the preferred metal for SPR biosensing because of its favorable combination of optical properties and chemical stability. However, other metals could be used, such as silver, copper, aluminum, and their combinations.[4−6,13] In addition, an increase in sensitivity and improvement in chemical properties has been achieved by depositing thin dielectric films on the metal surface[7] or by exploiting long-range surface plasmons.[8] To functionalize the metal surfaces, two primary linking layers are used: self-assembled monolayers and polymeric structures.[9−12] Self-assembled monolayers are usually formed using thiolated organic molecules that have a high affinity to gold. On the other hand, three-dimensional polymeric structures help to increase number of adsorption sites, among which dextran is the most popular material in commercial SPR systems.[9] However, in the last several years, much attention has been devoted to the usage of new carbon materials such as graphene and its oxidized counterpart, graphene oxide (GO), in the linking layers of SPR sensor chips.[14−24]

Graphene and graphene oxide are very promising materials for biosensors due to their high surface area, low-cost fabrication, and direct interaction with a wide range of biomolecules.[25−29] Moreover, graphene and graphene oxide can be processed in aqueous and organic solvents and prevent silver and copper films from oxidation.[15,30] Graphene is composed of carbon atoms arranged in a two-dimensional (2D) honeycomb lattice with sp2-hybridization, which can be used for biomolecule immobilization via pi-stacking.[25]

Received: May 21, 2015
Accepted: September 11, 2015
Published: September 11, 2015

DOI: 10.1021/acsami.5b04427
ACS Appl. Mater. Interfaces 2015, 7, 21727−21734

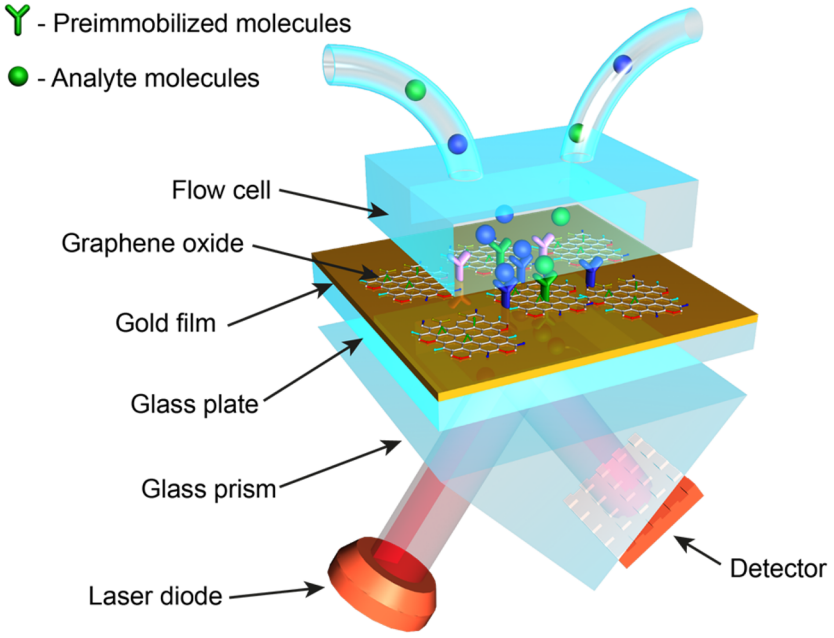

Figure 1. Schematic representation of the SPR biosensor comprising the SPR sensor chip with the graphene-oxide-linking layer, which forms in conjunction with the preimmobilized molecules that are highly selective to analyte.

Graphene oxide possesses both sp2- and sp3-hybridized carbon atoms as well as different functional groups such as epoxy, carboxyl, hydroxyl, and so on, which also enables covalent immobilization of biomolecules.[26−29] Moreover, compared to graphene, GO is dispersible in water and suitable for mass-production.[26] Furthermore, the GO chemical structure can be modified using thermal, chemical, or solvothermal reduction methods,[31] which could also be valuable for optical biosensors because the electronic and optical properties of GO can be tuned.

Graphene and GO have been both theoretically and experimentally investigated for applications in SPR biosensors and proven to enhance their performance.[32] According to the theory, the sensitivity of SPR biosensing is proportional to the thickness of the graphene film deposited on the surface of the sensor chip.[14] Graphene-based layers on gold surfaces serve as linking layer for biomolecules and can increase the sensitivity of biosensing by several times.[16] Deposition of graphene and GO layers on SPR sensor chips can be realized by several techniques. Monolayer graphene grown by chemical vapor deposition (CVD) can be transferred from the surface of the nickel or copper foil using thermal release tape[16] or spin-coated PMMA transfer film.[33] Other relatively simple, cost-effective methods for forming carbon layers include electrodeposition[19,20,34] and spin-coating[24] of water-soluble flakes of GO. Furthermore, some studies report the assembly of graphene and GO on the gold surface and the layers of thiols or cysteine molecules adsorbed on the gold surface.[17,18,22,23,35] In SPR applications, biomolecules can be immobilized on the surface of graphene or GO through the pi-stacking interaction[16,19,20] or through covalent conjugation between the carboxyl groups of GO and amino groups of these molecules.[17,18,22,23] Selective SPR biosensing of proteins and bacteria based on graphene has been demonstrated.[19,20]

In the present work, we propose patented highly sensitive and selective sensor chips utilizing GO thin films as the linking layers for biomolecule adsorption (Figure 1).[36] The GO was deposited on the surface of the gold layer with an airbrushing technique, which provides highly homogeneous films with controlled thickness over a wide range. Moreover, GO can be airbrushed on SPR sensor chips without its chemical reduction, which is an essential part of electrophoretic deposition.[37,38] In comparison to spin-coating method and deposition via self-assembly of GO flakes, the advantages of airbrushing technique are represented by thickness control and uniformity of obtained films.[39] The optical and morphological properties of the airbrushed GO films were investigated by spectroscopic ellipsometry[40] and atomic force microscopy (AFM).[41] The obtained properties were subsequently used for the analytical analysis of SPR in such multilayered structures and comparison of sensor chips based on graphene and GO. As a model experiment, we developed a highly sensitive and selective biosensing assay based on streptavidin (SA) molecules, which allows selective immobilization of biomolecules having biotin residue. The performance of the obtained sensor chips was evaluated in the analysis of DNA−DNA interactions, which could be valuable in various applications (e.g., with genotyping[42] and aptamers[43]). The proposed scheme shows higher sensitivity and a reduced signal-to-noise ratio due to its higher binding capacity in comparison to graphene-based and commercial sensor chips coated with carboxymethylated dextran. In addition, the developed sensor chips can be used multiple times following a simple regeneration procedure.

2. MATERIALS AND METHODS

2.1. Materials. An aqueous solution of GO with a concentration of 500 μg/mL was purchased from Graphene Laboratories, Inc. (NY, USA)[44] and was synthesized by Hummers method.[45] The GO solution contains at least 80% of one-atomic-layer flakes with a size of 0.3−0.7 μm, and the composition is 79% carbon and 20% oxygen. The GO films were airbrushed from the solution on two types of substrates: (1) a glass plate for ellipsometry measurements, and (2) gold sensor chips purchased from BiOptix, Inc. (Boulder, USA). Before deposition, the surfaces were cleaned for 10 min in the 3:1 Piranha solution of hydrogen peroxide and sulfuric acid. After cleaning, the surfaces were rinsed in water and dried under a stream of nitrogen. The substrate for film deposition was placed on a hot plate at 130 °C. Then, GO was

DOI: 10.1021/acsami.5b04427
ACS Appl. Mater. Interfaces 2015, 7, 21727−21734

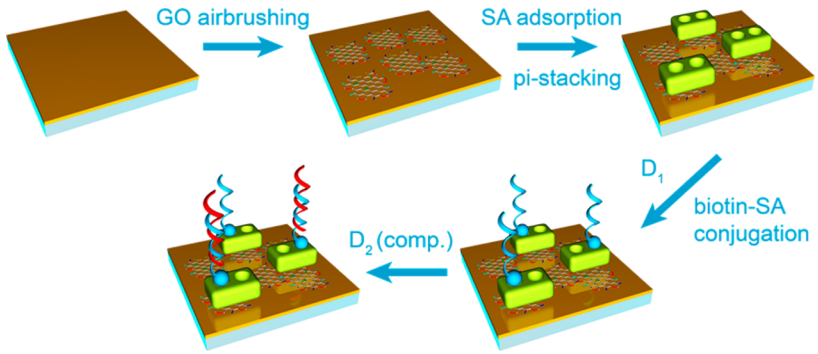

Figure 2. Schematic illustration of the procedure for detection of the interaction between the two complementary single-stranded oligonucleotide sequences.

sprayed on the substrate using the airbrushing technique with nitrogen as carrier gas at 2 bar.[46]

Monolayer graphene CVD grown on a copper foil of 20-μm thickness was purchased from Graphene Laboratories, Inc. (NY, USA). The graphene film was transferred on the surface of gold sensor chips using poly(methyl methacrylate) (PMMA) as an intermediate membrane.[47,48] PMMA was spin-coated by spin-coater Laurell Model WS-650Mz-23NPP at 2000 rpm for 1 min. After that PMMA was baked at 150 °C for 2 min. The 4% solution of 950 PMMA A4 in anisole was purchased from MicroChem Corp., USA. The Cu substrate under the graphene film was etched away in the 0.1 M ammonium persulfate solution in water during 6 h. The PMMA/graphene stack was washed in deionized water and placed onto the gold sensor chip. The obtained sensor chip was dried at 90 °C for 10 min. The PMMA film was then dissolved in acetone.

The oligonucleotides used in this study were synthesized by Integrated DNA Technologies (Corallville, USA) and included the biotinylated 56bp single-stranded DNA sequence (D_1) (5′-/5Biosg/TCT CTC TGA GTG GCC AAA ATT TCA TCT CTG AAT TCA GGG ATG ATG ATA ACA AAT GC-3′) and the 50bp single-stranded DNA sequence (D_2) (5′-GCA TTT GTT ATC ATC ATC CCT GAA TTC AGA GAT GAA ATT TTG GCC ACT CA-3′). Streptavidin was purchased from Thermo Scientific Pierce (Rockford, USA). All other chemicals were purchased from Sigma-Aldrich (Carlsbad, CA). The running buffer for SPR experiments was 0.1-M phosphate-buffered saline (PBS) with a pH of 7.4. The solution of streptavidin had a concentration of 100 μg/mL streptavidin in 50 mM of sodium acetate buffer with a pH of 4.5. For SPR instrument calibration, a 0.5% NaCl solution in running buffer was used. In the experiments, a 100 nM oligos solution in running buffer was used. The surfaces of the sensor chip were regenerated using 20 mM NaOH aqueous solutions. All solutions were prepared in ultrapure water with 18.3 MOhm cm.

2.2. Ellipsometry and Analytical Analysis. Both AFM imaging and spectroscopic ellipsometry were used to investigate the optical properties of GO films. The GO film was deposited on the surface of the glass slide by airbrushing. The surface coverage of GO flakes on the substrate was analyzed by scanning electron microscopy (SEM) (JEOL JSM-7001F). The refractive index (RI) of a slide is $n_{glass} = 1.458 + 5.09 \times 10^{-3}/\lambda^2$. The thickness of the GO film was obtained using AFM Ntegra Aura produced by NT-MDT (Moscow, Russia). The ellipsometry measurements were performed with the spectroscopic ellipsometer SE 800 (Sentech, Berlin, Germany). Xenon lamp illumination was used for measurements conducted in the wavelength range of 380−800 nm, and the angle of incidence of the light beam was 55°. The ellipsometric parameters Ψ and Δ obtained by measurements are defined as $r_p/r_s = \tan(\Psi)e^{i\Delta}$, where r_p and r_s are the reflection coefficients for the light with p and s polarizations, respectively. The complex refractive index of GO is modeled by the empirical Cauchy's equation, which accurately describes the optical properties of a material in the region of normal dispersion and presents the dependence of the real n_{GO} and imaginary k_{GO} parts of the refractive index on the wavelength λ in units of nanometers[49]

$$\begin{cases} n_{GO} = n_0 + (1 \times 10^2)n_1/\lambda^2 + (1 \times 10^7)n_2/\lambda^4 \\ k_{GO} = k_0 + (1 \times 10^2)k_1/\lambda^2 + (1 \times 10^7)k_2/\lambda^4 \end{cases} \quad (1)$$

where the constants n_0, n_1, n_2, k_0, k_1, and k_2 are reconstructed by numerical fitting from the experimental spectra. Fitting of the ellipsometric data was performed in SpectraRay 2 (Sentech, Berlin, Germany).

The obtained refractive index can be used to analyze the SPR reflectivity by the matrix method, describing the light reflection from the multilayered structure comprising GO.[50] The amplitude of the tangential fields (electric and magnetic fields in the cases of s- and p-polarizations of the incoming radiation, respectively) of transmitted A_i in the i-layer and reflected B_i from the i-layer radiation are connected with the same amplitudes in the $(i-1)$-layer by the following expression

$$\begin{pmatrix} A_i \\ B_i \end{pmatrix} = \frac{1}{t_{i,i-1}} \begin{pmatrix} e^{ik_i^z d_i} & 0 \\ 0 & e^{-ik_i^z d_i} \end{pmatrix} \begin{pmatrix} 1 & r_{i,i-1} \\ r_{i,i-1} & 1 \end{pmatrix} \begin{pmatrix} A_{i-1} \\ B_{i-1} \end{pmatrix} = M_i \begin{pmatrix} A_{i-1} \\ B_{i-1} \end{pmatrix} \quad (2)$$

where k_i^z is the projection of wavevector in the i-layer on the normal direction, d_i is the thickness of the i-layer, and $r_{i,i-1}$ and $t_{i,i-1}$ are the reflection and transmission coefficients for the considered field from $(i-1)$-layer to i-layer, respectively. For light transmitted from media with dielectric permittivity ε_1 to media with dielectric permittivity ε_2, the reflection and transmission coefficients are equal to

$$r_p = \frac{k_f^z - k_t^z}{k_f^z + k_t^z}, \; t_p = \frac{2k_f^z}{k_f^z + k_t^z} \quad (3)$$

for the p-polarization and

$$r_s = \frac{\varepsilon_2 k_f^z - \varepsilon_2 k_t^z}{\varepsilon_2 k_f^z + \varepsilon_2 k_t^z}, \; t_s = \frac{2\varepsilon_2 k_f^z}{\varepsilon_2 k_f^z + \varepsilon_2 k_t^z} \quad (4)$$

for the s-polarization, respectively. The analytical analysis of SPR in multilayered structures composing graphene and GO films was performed in MATLAB, Mathwork Inc., USA.

2.3. SPR Measurements. All SPR measurements were performed with an Accolade 404SA biosensor produced by the company BiOptix (Boulder, USA). This sensor exploits the Kretschmann configuration with surface plasmons excited by a laser diode at a wavelength of 635 nm. The sample solution is placed in contact with the sensing surface inside the flow cell, which operates at a constant temperature with a controlled flow rate. All experiments were conducted at 20 °C, and the flow rate for all solutions was 60 μL/min. For measurements, we used two types of sensor chips produced by BiOptix: pure gold sensor chips and chips with a carboxymethylated dextran (CMD) layer. The pure gold sensor chip comprises a plate of borosilicate glass covered with a titan adhesion layer and a thin gold layer. The CMD sensor chips are based on the carboxymethylated dextran layer with a thickness of 100 nm linked to the surface of a bare gold chip.

DOI: 10.1021/acsami.5b04427
ACS Appl. Mater. Interfaces 2015, 7, 21727−21734

To investigate the biochemical reactions, we coated the surfaces of CMD, graphene, and GO sensor chips with streptavidin (SA) protein for the subsequent immobilization of biotinylated samples. The protein solution with a concentration of 100 μg/mL was directly injected into the flow cell of the SPR instrument. For preparation of the GO sensor chips, we airbrushed 300 μL of GO solution with a concentration of 500 μg/mL. Streptavidin adsorption on the surfaces of the graphene and GO sensor chips was realized by a series of four 30 min injections of SA solution, and each injection was followed by 30 min of washing in the running buffer to remove weakly adsorbed molecules. This procedure allows the occupation of more adsorption sites on the GO surface. Streptavidin was adsorbed on the surface of the CMD sensor chip by amino-coupling. As a first step in amino-coupling reaction, we activated the carboxyl groups of CMD sensor chip with a mixture of 0.4-M 1-ethyl-3-(3-(dimethylamino)propyl) carbodiimide hydrochloride (EDC) and 0.1-M *N*-Hydroxysuccinimide (NHS) solutions in the 4-morpholineethanesulfonic acid (MES) buffer with a pH of 6.0 for 5 min. The EDC and NHS were mixed immediately before their injection in the flow cell of the SPR instrument. Then, streptavidin solution was injected at 5 min. Finally, the sensor chip surface was deactivated with 1 M ethanolamine solution at 5 min.

To evaluate the performance of the GO-SA sensor chips, we conducted a model experiment of the interaction of the complementary sequences of oligonucleotides D_1 and D_2, where D_1 is biotinylated (Figure 2). D1 was adsorbed on the surface of the sensor chip via interaction of its biotin residue with the streptavidin molecules immobilized on the surface of GO. The oligonucleotide solutions were diluted in a PBS running buffer with a concentration of 100 nM. Regeneration of the GO sensor chips was performed with a 20 nM solution of NaOH, which completely breaks the hydrogen bonds that hold complementary oligonucleotides together.

3. RESULTS AND DISCUSSION

3.1. Optical and Morphological Properties of GO Films. For ellipsometry measurements, 0.78 mL of 500 μg/mL GO solution was airbrushed on the surface of the glass slide. AFM analysis of this film gives the following values: thickness of 23 nm and a root-mean-squared roughness of 4.7 nm. Figure 3 shows the SEM image of the GO sensor chip and the AFM image of the scratch made on the GO film deposited on the glass substrate.

Figure 4a shows the spectroscopic ellipsometric data (Ψ and Δ) of the obtained GO film and the results of their fitting based on the refractive index for the substrate materials $n_{glass}(\lambda) = 1.458 + 5090/\lambda(\text{nm})^2$ and Cauchy's eq 1 for graphene oxide. We obtained $n_0 = 1.751$, $n_1 = 314.7$, $n_2 = -107.6$, $k_0 = 0.319$, $k_1 = -845.3$, and $k_2 = 1213.2$. Figure 4b presents the refractive index of GO sputtered by airbrushing and the refractive index of graphene, which is equal to $n_{gr} = 3 + i(1.82\lambda)$.[51] At the 635 nm wavelength of the SPR instrument light source, the imaginary part of the refractive index of graphene is six times smaller than that for GO, which gives the lower level of the surface plasmon adsorption and can be used to improve the biosensing sensitivity. Moreover, the optical and electronic properties of GO depend on its oxygen content and can be tuned by reduction for specific applications.[52,53]

3.2. SPR in the GO Systems. To estimate the influence of the GO and graphene layers, we performed numerical modeling of SPR in multilayer structures consisting of the following three layers: borosilicate glass with refractive index $n_1 = 1.723$, gold film with thickness of $d_2 = 50$ nm and refractive index $n_1 = 0.18016 + 3.4531i$,[54] and GO, graphene, or an aqueous solution comprising the third layer. An aqueous solution with refractive index $n_3 = 1.33$ is above the structure. The wavelength of the excitation light source is 635 nm.

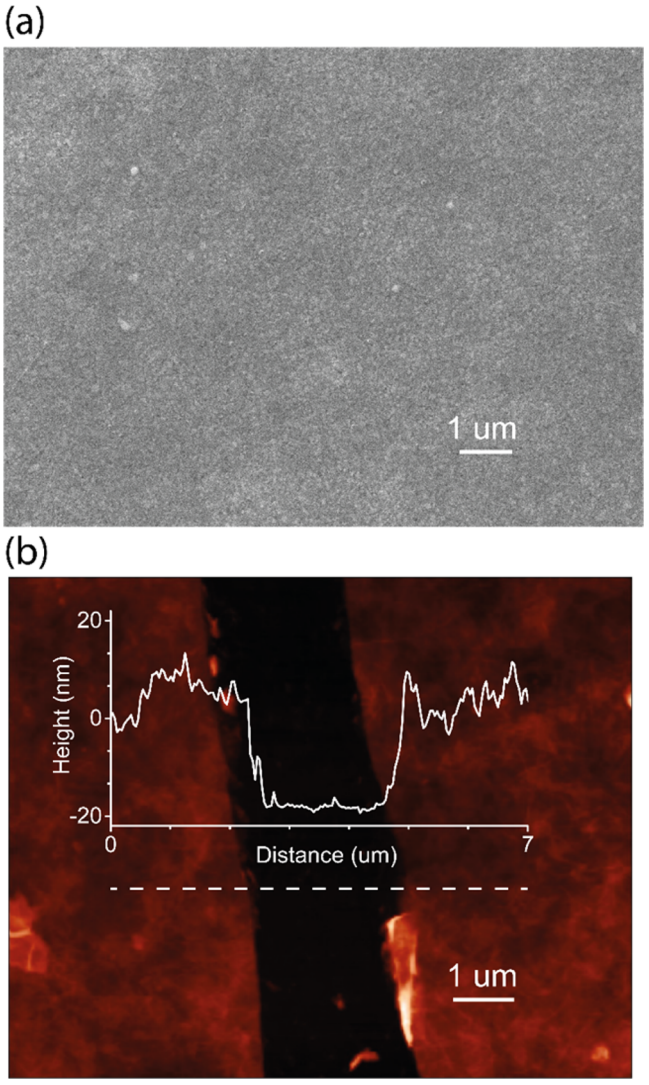

Figure 3. (a) SEM image of the GO sensor chip and (b) the AFM image of the scratch on the GO film deposited on the surface of the glass substrate. The GO film was deposited on the surface of the substrates from the aqueous solution with 500 μg/mL concentration of GO flakes. The volume of the deposited solutions was 0.78 mL. (b) Height profile of the scratched GO film.

The performance of the SPR biosensor is determined by the sensitivity, which is defined as the ratio of the change in the output signal to the changes in the measurement quantity.[3] For the most popular SPR biosensor based on Kretschmann's scheme[55] in which the output signal is SPR angle P and the measuring quantity is the analyte concentration C, the sensitivity is given by

$$S = \frac{\Delta P}{\Delta C} = \frac{\Delta P}{\Delta n}\frac{\Delta n}{\Delta C} = S_{RI}E \quad (5)$$

where Δn is the corresponding refractive index change, which is taken as 0.005 for modeling. Therefore, the sensitivity is decomposed in two parts: sensitivity to refractive index changes S_{RI} and efficiency E. The efficiency depends on the properties of the sensing surface and the type of analyte molecule and is proportional to the number of binding cites on the sensing surface $E \propto N_B$.

Figure 5a shows the shift of SPR curves with the change of the refractive index of the sensing medium from 1.33 (dashed)

DOI: 10.1021/acsami.5b04427
ACS Appl. Mater. Interfaces 2015, 7, 21727−21734

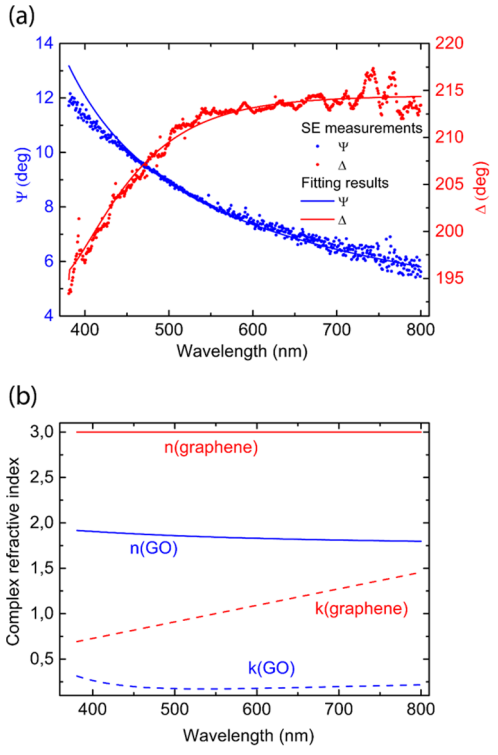

Figure 4. (a) Ellipsometric parameters Ψ and Δ (dotted lines) of the thin GO film deposited on a glass substrate, and the numerical fitting these parameter using the Cauchy's eq 1 for the modeling of the refractive index of the GO film (solid lines). (b) Real (solid lines) and imaginary (dashed lines) parts of the refractive indexes of graphene and GO.

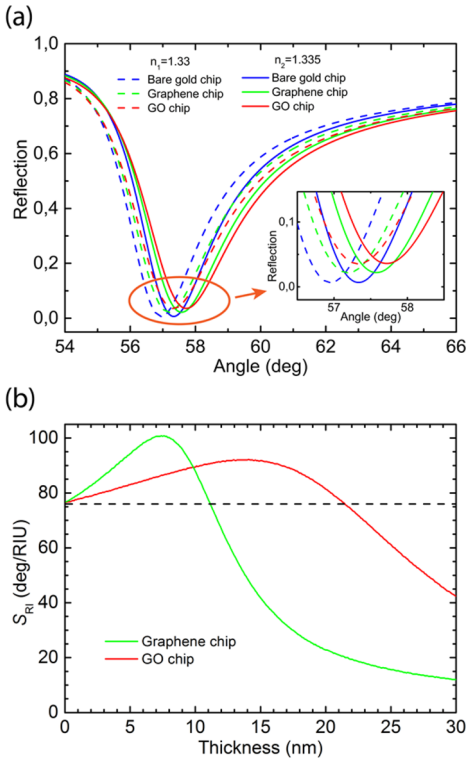

Figure 5. (a) SPR curves of the bare gold sensor chip (blue) and the gold sensor chips covered by monolayer graphene (green) and GO (red) for the two sensing medium with the refractive indices of 1.33 (dashed) and 1.335 (solid). (b) The sensitivity to the refractive index changes of the SPR biosensor chips based on GO and graphene. The dashed line shows the sensitivity of the bare gold SPR sensor chip to RI changes.

to 1.335 (solid) obtained for the bare gold sensor chip (blue) and the gold sensor chips covered by monolayer graphene (green) with the thickness of 0.34 nm and GO (red) with the thickness of 1 nm. According to the eq 5, the difference between SPR angles induced by this shift is proportional to the sensitivity to refractive index changes S_{RI}. Figure 5b shows the dependencies of S_{RI} for gold sensor chips covered by graphene and GO on the thicknesses of these layers, where the dashed line corresponds to the sensitivity to refractive index changes S^0_{RI} = 76.6 deg/RIU of the bare gold chip. Graphene-based sensor chips show an increase in sensitivity to RI changes for layers up to 11 nm in thickness with a maximum of 101 deg/RIU at 7 nm, which is 32% higher than that of the bare gold chip. Further increase of the graphene layer thickness leads to the rapid decrease of S_{RI}, lowering to 12 deg/RIU at 30 nm. The influence of GO thin films deposited on the surface of a sensor chip is weaker with a peak sensitivity to RI changes of 92 deg/RIU (S_{RI}/S^0_{RI} = 120%) at 14 nm GO film thickness, which decreases to 42.4 deg/RIU at 30 nm.

The thickness of the graphene films composing the SPR sensor chips is strongly limited by optical absorption, which leads to the reduction of sensitivity for films with thicknesses higher than 10 nm. However, the surface plasmon penetration depth into the solution at the excitation wavelength of 635 nm is about 490 nm,[56] which defines a region near the sensor chip surface where biomolecule binding could be detected. The usage of GO as a linking layer for biomolecules allows the usage of thicker films with a larger number of binding sites due to the low optical adsorption of graphene oxide. An additional increase of sensitivity to the refractive changes S_{RI} could be reached by proper oxidation of GO, which changes its optical properties, and by carbon-porous-structure-based linking layers,[57] which decrease surface plasmon attenuation and could be permeable to biomolecules. Furthermore, the possibility of using thicker linking layers (with thickness up to hundreds of nanometers) could help dramatically increase sensor efficiency E due to the increased surface area.

3.3. GO Sensor Chip Based on Biotin–Streptavidin Complex. We used SPR sensor chips based on two different types of linking layers to create biosensing assays based on streptavidin molecules. We considered a commercial sensor chip comprising a 100 nm thick layer of CMD, a pure gold chip covered by monolayer graphene, and a pure gold chip covered by the airbrushed layer of graphene oxide with a thickness of ~8.8 nm, which gives a 15% increase in sensitivity to refractive index changes S_{RI}. Streptavidin was immobilized on the surface of the CMD chip by amino-coupling procedure (Figure 6a), during which SA bonded covalently to the 3D polymer hydrogel. The SPR signal corresponding to the adsorption of streptavidin on the CMD sensor chip was 1270 RU. The adsorption of streptavidin on monolayer graphene and GO was performed directly in the flow cell of the SPR instrument without any additional chemistry. During four consecutive adsorptions (Figure 6b), the SPR signals were 500 RU, 220 RU, 120 RU, and 140 RU respectively. The SPR signal corresponding to the total amount of SA adsorbed on the graphene surface is 980 RU. In the case of SA adsorption on the surface of GO, the SPR signal were 1600 RU, 840 RU, 400 RU, and 350 RU resulting in the total SPR signal of 3190 RU. The

DOI: 10.1021/acsami.5b04427
ACS Appl. Mater. Interfaces 2015, 7, 21727–21734

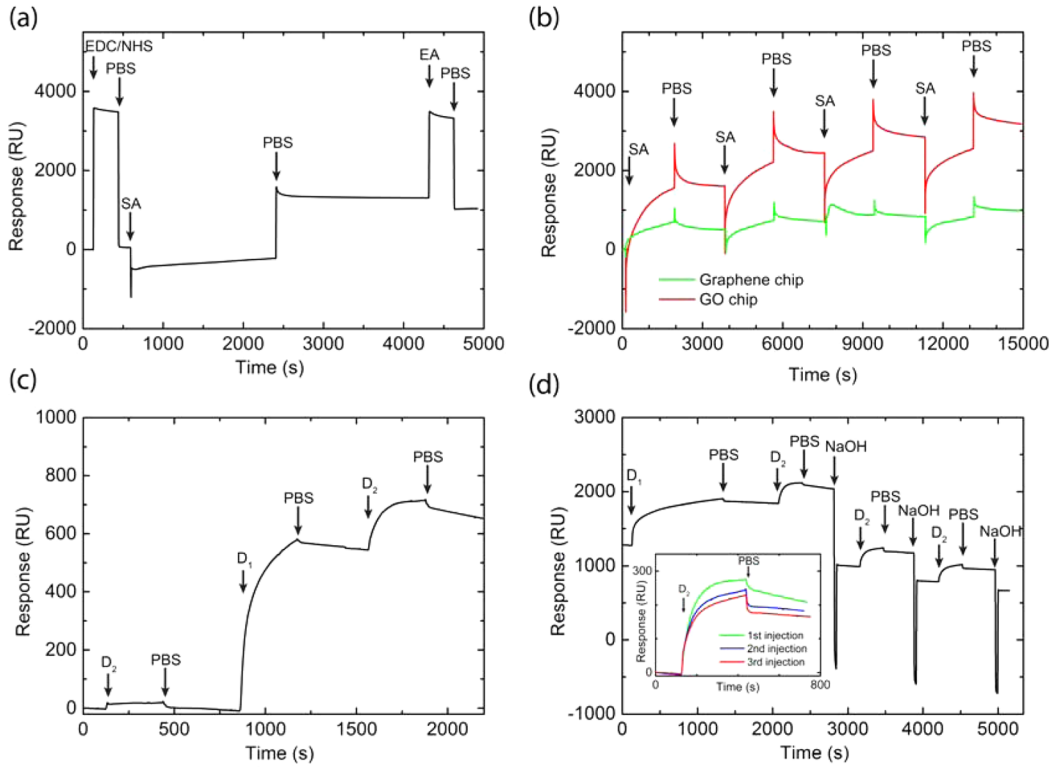

Figure 6. SA adsorption from the 100 μg/mL solution (a) on the sensor chip based on CMD using the amino-coupling procedure and (b) on the sensor chip covered by monolayer graphene (green) and airbrushed GO film (red) through pi-stacking interaction. (c) Adsorption of the oligonucleotide sequences D_1 and D_2 on the SA-GO sensor chip, where D_1 is biotinylated and D_2 is nonbiotinylated and complementary to D_1. (d) The regeneration of the SA-GO sensor chip using a 20-mM solution of NaOH, which breaks the hydrogen bonds between the complementary DNA strands D_1 and D_2. Therefore, after NaOH injection, D_2 is eluted, leaving D_1 attached to streptavidin.

relative decrease in the amount of the adsorbed proteins on the surfaces of graphene and GO shows gradual depletion of the adsorption sites on the GO surface. The SPR signal corresponding to the SA adsorbed on the GO surface is 250 and 325% of the SA adsorbed on the CMD and graphene sensor chips, respectively. Higher amount of adsorbed streptavidin provides more adsorption sites for the analyte molecules, increasing efficiency E of the recognition surface by approximately 2.5 times and 3.25 times comparing to the surfaces of CMD and graphene sensor chips, respectively. According to eq 5, we determine that the GO sensor chips were 2.9 times more sensitive than the CMD chips and 3.7 times more sensitive than the graphene chips.

The GO linking layer, which is deposited on the top of the gold film, is much thinner compared to the CMD layer, which is good for applications with viruses, cells, and big proteins. Moreover, for applications with small molecules, there is a possibility for further improvement of the sensitivity with the creation of 3D structures based on GO. In addition, the sensogram in Figure 6b indicates a large amount of SA desorption during PBS washing during each adsorption step, which arises because of the relatively weak bond between the aromatic rings of biomolecules and graphene flakes. To improve biomolecule immobilization, streptavidin and other biological samples that are interesting for SPR applications can be covalently adsorbed on the surface of GO using its functional groups.[28]

The obtained sensor chips based on airbrushed GO films are biospecific and interact only with biomolecules having biotin residue. Figure 6c shows consecutive adsorptions of oligonucleotide sequences D_2, D_1, and D_2. Only D_1 is biotinylated, and D_2 is complementary to D_1. The first adsorption of D_2 is negligible with an SPR signal less than 5 RU, whereas the SPR signals for the D_1 adsorption and the second D_2 adsorption due to complementary strand interactions are 560 RU and 140 RU, respectively. Therefore, we determine that the nonspecific DNA adsorption is less than 4% compared to the specific interaction, which demonstrates that SPR sensor ships based on GO-streptavidin biolayers are biospecific.

Moreover, GO sensor chips for the analysis of DNA interaction could be used multiple times using a simple procedure of regeneration using a 20-mM solution of NaOH, which forms a high pH environment in the flow cell and breaks hydrogen bonds between complementary DNA strands. After NaOH injection, D_2 is eluted, leaving D_1 attached to streptavidin. Figure 6d presents the kinetic curve of three consecutive adsorptions of D_2 followed by the regeneration procedure. The amount of D_2 adsorbed in the subsequent tests is 240 RU, 195 RU, and 175 RU, respectively, with repeatability of the adsorptions in the range of 10−25%.

4. CONCLUSION

We have proposed highly sensitive and selective SPR sensor chips with linking layers based on airbrushed GO films. For airbrush deposition, we used GO flakes processed in an aqueous solution, which are inexpensive and suitable for mass production. The obtained GO films are highly homogeneous with roughness of several nanometers with a thickness defined by the amount of used GO solution. The optical properties of the obtained GO films were investigated by means of

DOI: 10.1021/acsami.5b04427
ACS Appl. Mater. Interfaces 2015, 7, 21727−21734

spectroscopic ellipsometry, showing much lower optical adsorption in the visible range than that of graphene. According to numerical simulations, the GO linking layers could have twice the thickness than those from graphene without loss of sensitivity. By optimizing the thickness of the GO film deposited on the surface of the gold film, we can reach a 20% increase in the sensitivity of the SPR biosensor to changes in the refractive index. Linking layers based on GO can be used for the development of different biosensing assays due to the possible GO interactions with different types of biomolecules via pi-stacking. As a model experiment, we realized a biosensing assay based on a biolayer comprising streptavidin, which can be used to investigate biomolecules with biotin residue. The amount of the deposited streptavidin is 2.5 times higher in the case of GO linking layers, than that for commercial sensor chips based on the three-dimensional carboxymethylated dextran with a 2.9 times higher biosensing sensitivity. Furthermore, the GO surface provides 3.25 times higher number of binding sites than the surface of monolayer graphene deposited on a gold chip using PMMA as an intermediate membrane. The biosensing sensitivity is 3.7 times higher for the GO chip than for the graphene chip. Nonspecific binding on the GO-streptavidin chip is less than 4% of the specific binding for used oligonucleotides. In addition, the obtained sensor chip can be used multiple times with 10−25% accuracy of repeatability. With further development, the proposed sensor chips could use porous-graphene-oxide films as linking layers that will potentially lead to greater adsorption efficiency and sensitivity. The results obtained demonstrate unique possibilities opening with the usage of GO chips for optical biosensing applications (e.g., including the possibility of using GO chips as a possible substitute for commercially available SPR sensor chips), even though the proposed GO sensor chip platform should still be carefully validated in a number of applications besides analysis of nucleic acid (e.g., investigations of biochemical reactions with different interaction partners, such as antigens, antibodies, receptors, drugs, viruses, cells, and others[12]).

AUTHOR INFORMATION

Corresponding Author

*E-mail: ystebunov@gmail.com.

Notes

The authors declare no competing financial interest.

ACKNOWLEDGMENTS

This work was supported by the Ministry of Education and Science of the Russian Federation (16.19.2014/K and CCU MIPT RFMEFI59414 × 0009). The authors thank Boris Khattatov and Slava Petropavlovskikh from the BiOptix, Inc (Boulder, USA) for expert technical assistance and helpful discussions with the experiment.

REFERENCES

(1) Karlsson, R. SPR for Molecular Interaction Analysis: A Review of Emerging Application Areas. *J. Mol. Recognit.* **2004**, *17* (3), 151−161.
(2) Fan, X.; White, I. M.; Shopova, S. I.; Zhu, H.; Suter, J. D.; Sun, Y. Sensitive Optical Biosensors for Unlabeled Targets: A Review. *Anal. Chim. Acta* **2008**, *620*, 8−26.
(3) Homola, J. Present and Future of Surface Plasmon Resonance Biosensors. *Anal. Bioanal. Chem.* **2003**, *377* (3), 528−539.
(4) Zhu, X. M.; Lin, P. H.; Ao, P.; Sorensen, L. B. Surface Treatments for Surface Plasmon Resonance Biosensors. *Sens. Actuators, B* **2002**, *84*, 106−112.
(5) Ong, B. H.; Yuan, X.; Tjin, S. C.; Zhang, J.; Ng, H. M. Optimized Film Thickness for Maximum Evanescent Field Enhancement of a Bimetallic Film Surface Plasmon Resonance Biosensor. *Sens. Actuators, B* **2006**, *114*, 1028−1034.
(6) Choi, S. H.; Byun, K. M. Investigation on an Application of Silver Substrates For Sensitive Surface Plasmon Resonance Imaging Detection. *J. Opt. Soc. Am. A* **2010**, *27* (10), 2229−2236.
(7) Lahav, A.; Auslender, M.; Abdulhalim, I. Sensitivity Enhancement of Guided-Wave Surface-Plasmon Resonance Sensors. *Opt. Lett.* **2008**, *33* (21), 2539−2541.
(8) Nenninger, G. G.; TobisÏka, P.; Homola, J.; Yee, S. S. Long-Range Surface Plasmons for High-Resolution Surface Plasmon Resonance Sensors. *Sens. Actuators, B* **2001**, *74*, 145−151.
(9) Johnsson, B.; Löfås, S.; Lindquist, G. Immobilization of Proteins to a Carboxymethyldextran-Modified Gold Surface for Biospecific Interaction Analysis in Surface Plasmon Resonance Sensors. *Anal. Biochem.* **1991**, *198* (2), 268−277.
(10) Schuck, P. Use of Surface Plasmon Resonance to Probe the Equilibrium and Dynamic Aspects of Interactions Between Biological Macromolecules. *Annu. Rev. Biophys. Biomol. Struct.* **1997**, *26*, 541−566.
(11) Scarano, S.; Mascini, M.; Turner, A. P. F.; Minunni, M. Surface Plasmon Resonance Imaging for Affinity-Based Biosensors. *Biosens. Bioelectron.* **2010**, *25* (5), 957−966.
(12) Samanta, D.; Sarkar, A. Immobilization of Bio-Macromolecules on Self-Assembled Monolayers: Methods and Sensor Applications. *Chem. Soc. Rev.* **2011**, *40* (5), 2567−2592.
(13) West, P. R.; Ishii, S.; Naik, G. V.; Emani, N. K.; Shalaev, V. M.; Boltasseva, A. Searching for Better Plasmonic Materials. *Laser Photonics Rev.* **2010**, *4* (6), 795−808.
(14) Wu, L.; Chu, H. S.; Koh, W. S.; Li, E. P. Highly Sensitive Graphene Biosensors Based on Surface Plasmon Resonance. *Opt. Express* **2010**, *18* (14), 14395−14400.
(15) Choi, S. H.; Kim, Y. L.; Byun, K. M. Graphene-on-Silver Substrates for Sensitive Surface Plasmon Resonance Imaging Biosensors. *Opt. Express* **2011**, *19* (2), 458−466.
(16) Wijaya, E.; Maalouli, N.; Boukherroub, R.; Szunerits, S.; Vilcot, J.-P. Graphene-Based High-Performance Surface Plasmon Resonance Biosensors. *Proc. SPIE* **2012**, *8424*, 84240R.
(17) Zhang, J.; Sun, Y.; Xu, B.; Zhang, H.; Gao, Y.; Zhang, H.; Song, D. A Novel Surface Plasmon Resonance Biosensor Based on Graphene Oxide Decorated with Gold Nanorod−Antibody Conjugates for Determination of Transferrin. *Biosens. Bioelectron.* **2013**, *45*, 230−236.
(18) Zhang, J.; Sun, Y.; Wu, Q.; Gao, Y.; Zhang, H.; Bai, Y.; Song, D. Preparation of Graphene Oxide-Based Surface Plasmon Resonance Biosensor with Au Bipyramid Nanoparticles as Sensitivity Enhancer. *Colloids Surf., B* **2014**, *116*, 211−218.
(19) Subramanian, P.; Lesniewski, A.; Kaminska, I.; Vlandas, A.; Vasilescu, A.; Niedziolka-Jonsson, J.; Pichonat, E.; Happy, H.; Boukherroub, R.; Szunerits, S. Lysozyme Detection on Aptamer Functionalized Graphene-Coated SPR Interfaces. *Biosens. Bioelectron.* **2013**, *50*, 239−243.
(20) Subramanian, P.; Barka-Bouaifel, F.; Bouckaert, J.; Yamakawa, N.; Boukherroub, R.; Szunerits, S. Graphene-Coated Surface Plasmon Resonance Interfaces for Studying the Interactions between Bacteria and Surfaces. *ACS Appl. Mater. Interfaces* **2014**, *6* (8), 5422−5431.
(21) Szunerits, S.; Maalouli, N.; Wijaya, E.; Vilcot, J.-P.; Boukherroub, R. Recent Advances in the Development of Graphene-Based Surface Plasmon Resonance (SPR) Interfaces. *Anal. Bioanal. Chem.* **2013**, *405*, 1435−1443.
(22) Chiu, N.-F.; Huang, T.-Y.; Lai, H.-C.; Liu, K.-C. Graphene Oxide-Based SPR Biosensor Chip for Immunoassay Applications. *Nanoscale Res. Lett.* **2014**, *9* (1), 445.
(23) Chiu, N.-F.; Huang, T.-Y. Sensitivity and Kinetic Analysis of Graphene Oxide-Based Surface Plasmon Resonance Biosensors. *Sens. Actuators, B* **2014**, *197*, 35−42.
(24) Lokman, N. F.; Bakar, A. A. A.; Suja, F.; Abdullah, H.; Ab Rahman, W. B. W.; Huang, N.-M.; Yaacob, M. H. Highly Sensitive

DOI: 10.1021/acsami.5b04427
ACS Appl. Mater. Interfaces 2015, 7, 21727−21734

SPR Response of Au/Chitosan/Graphene Oxide Nanostructured Thin Films Toward Pb (II) Ions. *Sens. Actuators, B* **2014**, *195*, 459−466.
(25) Morales-Narváez, E.; Merkoçi, A. Graphene Oxide as an Optical Biosensing Platform. *Adv. Mater.* **2012**, *24* (25), 3298−3308.
(26) Dreyer, D. R.; Park, S.; Bielawski, C. W.; Ruoff, R. S. The Chemistry of Graphene Oxide. *Chem. Soc. Rev.* **2010**, *39*, 228−240.
(27) Chen, D.; Feng, H.; Li, J. Graphene Oxide: Preparation, Functionalization, and Electrochemical Applications. *Chem. Rev.* **2012**, *112* (11), 6027−6053.
(28) Georgakilas, V.; Otyepka, M.; Bourlinos, A. B.; Chandra, V.; Kim, N.; Kemp, K. C.; Hobza, P.; Zboril, R.; Kim, K. S. Functionalization of Graphene: Covalent and Non-Covalent Approaches, Derivatives and Applications. *Chem. Rev.* **2012**, *112* (11), 6156−6214.
(29) Wang, Y.; Li, Z.; Wang, J.; Li, J.; Lin, Y. Graphene and Graphene Oxide: Biofunctionalization and Applications in Biotechnology. *Trends Biotechnol.* **2011**, *29* (5), 205−212.
(30) Kravets, V. G.; Jalil, R.; Kim, Y.-J.; Ansell, D.; Aznakayeva, D. E.; Thackray, B.; Belle, B. D.; Withers, F.; Radko, I. P.; Han, Z.; Bozhevolnyi, S. I.; Novoselov, K. S.; Geim, A. K.; Grigorenko, A. N. Graphene-Protected Copper and Silver Plasmonics. *Sci. Rep.* **2014**, *4*, 5517.
(31) Pei, S.; Cheng, H.-M. The Reduction of Graphene Oxide. *Carbon* **2012**, *50* (9), 3210−3228.
(32) Ferrari, A. C.; Bonaccorso, F.; Fal'ko, F.; Novoselov, K. S.; Roche, S.; Bøggild, P.; Borini, S.; Koppens, F. H. L.; Palermo, V.; Pugno, N.; Garrido, J. A.; Sordan, R.; Bianco, A.; Ballerini, L.; Prato, M.; Lidorikis, E.; Kivioja, J.; Marinelli, C.; Ryhänen, T.; Morpurgo, A.; Coleman, J. N.; Nicolosi, V.; Colombo, L.; Fert, A.; Garcia-Hernandez, M.; Bachtold, A.; Schneider, G. F.; Guinea, F.; Dekker, C.; Barbone, M.; Sun, Z.; Galiotis, C.; Grigorenko, A. N.; Konstantatos, G.; Kis, A.; Katsnelson, M.; Vandersypen, L.; Loiseau, A.; Morandi, V.; Neumaier, D.; Treossi, E.; Pellegrini, V.; Polini, M.; Tredicucci, A.; Williams, G. M.; Hong, B. H.; Ahn, J.-H.; Kim, J. M.; Zirath, H.; van Wees, B. J.; van der Zant, H.; Occhipinti, L.; Matteo, A. D.; Kinloch, I. A.; Seyller, T.; Quesnel, E.; Feng, X.; Teo, K.; Rupesinghe, N.; Hakonen, P.; Neil, S. R. T.; Tannock, Q.; Löfwanderaq, T.; Kinaret, J. Science and Technology Roadmap for Graphene, Related Two-Dimensional Crystals, and Hybrid Systems. *Nanoscale* **2015**, *7* (11), 4598−4810.
(33) Penezic, A.; Deokar, G.; Vignaud, D.; Pichonat, E.; Happy, H.; Subramanian, P.; Gasparović, B.; Boukherroub, R.; Szunerits, S. Carbohydrate−Lectin Interaction on Graphene-Coated Surface Plasmon Resonance (SPR) Interfaces. *Plasmonics* **2014**, *9* (3), 677−683.
(34) Xue, T.; Cui, X.; Guan, W.; Wang, Q.; Liu, C.; Wang, H.; Qi, K.; Singh, D. J.; Zheng, W. Surface Plasmon Resonance Technique for Directly Probing the Interaction of DNA and Graphene Oxide and Ultra-Sensitive Biosensing. *Biosens. Bioelectron.* **2014**, *58*, 374−379.
(35) Song, B.; Li, D.; Qi, W.; Elstner, M.; Fan, C.; Fang, H. Graphene on Au(111): A Highly Conductive Material with Excellent Adsorption Properties for High-Resolution Bio/Nanodetection and Identification. *ChemPhysChem* **2010**, *11* (3), 585−589.
(36) Arsenin, A. V.; Stebunov, Yu.V. RU Patent Application No. 2527699 (Feb 2013); WO/2014/129933 International Application No. PCT/RU2013/001100 (Aug 2014).
(37) An, S. J.; Zhu, Y.; Lee, S. H.; Stoller, M. D.; Emilsson, T.; Park, S.; Velamakanni, A.; An, J.; Ruoff, R. S. Thin Film Fabrication and Simultaneous Anodic Reduction of Deposited Graphene Oxide Platelets by Electrophoretic Deposition. *J. Phys. Chem. Lett.* **2010**, *1*, 1259−1263.
(38) Koh, A. T. T.; Foong, Y. M.; Pan, L.; Sun, Z.; Chua, D. H. C. Effective Large-Area Free-Standing Graphene Field Emitters by Electrophoretic Deposition. *Appl. Phys. Lett.* **2012**, *101*, 183107.
(39) Guo, Y.; Di, C.; Liu, H.; Zheng, J.; Zhang, L.; Yu, G.; Liu, Y. General Route toward Patterning of Graphene Oxide by a Combination of Wettability Modulation and Spin-Coating. *ACS Nano* **2010**, *4*, 5749−5754.
(40) Fujiwara, H. *Spectroscopic Ellipsometry: Principles and Applications*; John Wiley & Sons: Tokyo, 2007.
(41) Binnig, G.; Quate, C. F.; Gerber, Ch. Atomic Force Microscope. *Phys. Rev. Lett.* **1986**, *56* (9), 930−934.
(42) Mariani, S.; Scarano, S.; Carrai, M.; Barale, R.; Minunni, M. Direct genotyping of C3435T single nucleotide polymorphism in unamplified human MDR1 gene using a surface plasmon resonance imaging DNA sensor. *Anal. Bioanal. Chem.* **2015**, *407* (14), 4023−4028.
(43) Song, S.; Wang, L.; Li, J.; Zhao, J.; Fan, C. Aptamer-based biosensors. *TrAC, Trends Anal. Chem.* **2008**, *27* (2), 108−117.
(44) https://graphene-supermarket.com/.
(45) Hummers, W. S.; Offeman, R. E. *J. Am. Chem. Soc.* **1958**, *80* (6), 1339.
(46) Tong, Y.; Bohm, S.; Song, M. Graphene Based Materials and Their Composites as Coatings. *Austin J. Nanomed. Nanotechnol.* **2014**, *1* (1), 1003.
(47) Li, X.; Zhu, Y.; Cai, W.; Borysiak, M.; Han, B.; Chen, D.; Piner, R. D.; Colombo, L.; Ruoff, R. S. Transfer of Large-Area Graphene Films for High-Performance Transparent Conductive Electrodes. *Nano Lett.* **2009**, *9*, 4359−4363.
(48) Liang, X.; Sperling, B. A.; Calizo, I.; Cheng, G.; Hacker, C. A.; Zhang, Q.; Obeng, Y.; Yan, K.; Peng, H.; Li, Q.; Zhu, X.; Yuan, H.; Walker, A. R. H.; Liu, Z.; Peng, L.; Richter, C. A. Toward Clean and Crackless Transfer of Graphene. *ACS Nano* **2011**, *5*, 9144−9153.
(49) Jenkins, F. A.; White, H. E. *Fundamentals of Optics*, fourth ed.; McGraw−Hill: New York, 2001.
(50) Yamamoto, M. Surface Plasmon Resonance (SPR) Theory: Tutorial. *Rev. Polarogr.* **2002**, *48* (3), 209−237.
(51) Bruna, M.; Borini, S. Optical Constants of Graphene Layers in the Visible Range. *Appl. Phys. Lett.* **2009**, *94* (3), 031901.
(52) Jung, I.; Vaupel, M.; Pelton, M.; Piner, R.; Dikin, D. A.; Stankovich, S.; An, J.; Ruoff, R. S. Characterization of Thermally Reduced Graphene Oxide by Imaging Ellipsometry. *J. Phys. Chem. C* **2008**, *112* (23), 8499−8506.
(53) Shen, Y.; Zhou, P.; Sun, Q. Q.; Wan, L.; Li, J.; Chen, L. Y.; Zhang, D. W.; Wang, X. B. Optical Investigation of Reduced Graphene Oxide by Spectroscopic Ellipsometry and the Band-Gap Tuning. *Appl. Phys. Lett.* **2011**, *99* (14), 141911.
(54) Johnson, P. B.; Christy, R. W. Optical Constants of the Noble Metals. *Phys. Rev. B* **1972**, *6*, 4370−4379.
(55) Kretschmann, E. Die Bestimmung optischer Konstanten von Metallen durch Anregung von Oberflachenplasmaschwingugnen. *Eur. Phys. J. A* **1971**, *241*, 313−324.
(56) Homola, J. *Surface Plasmon Resonance Based Sensors*. Springer Series on Chemical Sensors and Biosensors; Springer−Verlag: Berlin, 2006; Vol. *4*.
(57) Zhu, J.; Chen, M.; He, Q.; Shao, L.; Wei, S.; Guo, Z. An Overview of the Engineered Graphene Nanostructures and Nanocomposites. *RSC Adv.* **2013**, *3* (45), 22790−22824.

DOI: 10.1021/acsami.5b04427
ACS Appl. Mater. Interfaces 2015, 7, 21727−21734